



Graded-Index Separated Confinement Heterostructure AlGaIn Nanowires: Towards Ultraviolet Laser Diodes Implementation

Item Type	Article
Authors	Sun, Haiding; Priante, Davide; Min, Jung-Wook; Subedi, Ram Chandra; Shakfa, Mohammad Khaled; Ren, Zhongjie; Li, Kuang-Hui; Lin, Ronghui; Zhao, Chao; Ng, Tien Khee; Ryou, Jae-Hyun; Zhang, Xixiang; Ooi, Boon S.; Li, Xiaohang
Citation	Sun H, Priante D, Min J-W, Subedi RC, Shakfa MK, et al. (2018) Graded-Index Separate Confinement Heterostructure AlGaIn Nanowires: Toward Ultraviolet Laser Diodes Implementation. ACS Photonics 5: 3305–3314. Available: http://dx.doi.org/10.1021/acsp Photonics.8b00538 .
Eprint version	Post-print
DOI	10.1021/acsp Photonics.8b00538
Publisher	American Chemical Society (ACS)
Journal	ACS Photonics
Rights	This document is the Accepted Manuscript version of a Published Work that appeared in final form in ACS Photonics, copyright © American Chemical Society after peer review and technical editing by the publisher. To access the final edited and published work see https://pubs.acs.org/doi/10.1021/acsp Photonics.8b00538 .
Download date	04/08/2022 16:22:01

Link to Item	http://hdl.handle.net/10754/628295
--------------	---

Graded-Index Separated Confinement Heterostructure AlGaIn Nanowires: Towards Ultraviolet Laser Diodes Implementation

Haiding Sun, Davide Priante, Jung-Wook Min, Ram Chandra Subedi, Mohammad Khaled Shakfa, Zhongjie Ren, Kuang-Hui Li, Ronghui Lin, Chao Zhao, Tien Khee Ng, Jae-Hyun Ryou, Xixiang Zhang, Boon S. Ooi, and Xiaohang Li

ACS Photonics, **Just Accepted Manuscript** • DOI: 10.1021/acsp Photonics.8b00538 • Publication Date (Web): 19 Jun 2018

Downloaded from <http://pubs.acs.org> on June 20, 2018

Just Accepted

"Just Accepted" manuscripts have been peer-reviewed and accepted for publication. They are posted online prior to technical editing, formatting for publication and author proofing. The American Chemical Society provides "Just Accepted" as a service to the research community to expedite the dissemination of scientific material as soon as possible after acceptance. "Just Accepted" manuscripts appear in full in PDF format accompanied by an HTML abstract. "Just Accepted" manuscripts have been fully peer reviewed, but should not be considered the official version of record. They are citable by the Digital Object Identifier (DOI®). "Just Accepted" is an optional service offered to authors. Therefore, the "Just Accepted" Web site may not include all articles that will be published in the journal. After a manuscript is technically edited and formatted, it will be removed from the "Just Accepted" Web site and published as an ASAP article. Note that technical editing may introduce minor changes to the manuscript text and/or graphics which could affect content, and all legal disclaimers and ethical guidelines that apply to the journal pertain. ACS cannot be held responsible for errors or consequences arising from the use of information contained in these "Just Accepted" manuscripts.

Graded-Index Separated Confinement Heterostructure AlGaN Nanowires: Towards Ultraviolet Laser Diodes Implementation

Haiding Sun^{1#}, Davide Priante², Jung-Wook Min², Ram Chandra Subedi², Mohammad Khaled Shakfa², Zhongjie Ren¹, Kuang-Hui Li¹, Ronghui Lin¹, Chao Zhao², Tien Khee Ng², Jae-Hyun Ryou³, Xixiang Zhang⁴, Boon S. Ooi^{2##}, Xiaohang Li^{1, ###}

¹ King Abdullah University of Science & Technology (KAUST), Computer, Electrical, and Mathematical Sciences and Engineering Division, Advanced Semiconductor Laboratory, Thuwal 23955-6900, Saudi Arabia
² King Abdullah University of Science & Technology (KAUST), Computer, Electrical, and Mathematical Sciences and Engineering Division, Photonics Laboratory, Thuwal 23955-6900, Saudi Arabia
³ Department of Mechanical Engineering, Material Science and Engineering Program, Texas Center for Superconductivity at UH (TcSUH), and Advanced Manufacturing Institute (AMI), University of Houston, Houston, TX, 77204-4006, USA
⁴ Division of Physical Science and Engineering, King Abdullah University of Science and Technology, Thuwal 23955-6900, Saudi Arabia

KEYWORDS

Aluminum gallium nitride nanowire, graded index, polarization doping, ultraviolet laser

Abstract

High-density dislocations in materials and poor electrical conductivity of p-type AlGaN layers constrain the performance of the ultraviolet light emitting diodes and lasers at shorter wavelengths. To address those technical challenges, we design, grow, and fabricate a novel nanowire structure adopting a graded-index separate confinement heterostructure (GRINSCH) in which the active region is sandwiched between two compositionally graded AlGaN layers, namely a GRINSCH diode. Calculated electronic band diagram and carrier concentrations show an automatic formation of a p-n junction with electron and hole concentrations of $\sim 10^{18}$ /cm³ in the graded AlGaN layers without intentional doping. The transmission electron microscopy experiment confirms the composition variation in the axial direction of the graded AlGaN nanowires. Significantly lower turn-on voltage of 6.5 V (reduced by 2.5 V) and smaller series resistance of 16.7 Ω (reduced by nearly four times) are achieved in the GRINSCH diode, compared with the conventional p-i-n diode. Such an improvement in the electrical performance is mainly attributed to the effectiveness of polarization-induced n- and p-doping in the compositionally graded AlGaN layers. In consequence, the carrier transport and injection efficiency of the GRINSCH diode are greatly enhanced, which leads to a lower turn-on voltage, smaller series resistance, higher output power, and enhanced device efficiency. The calculated carrier distributions (both

electrons and holes) across the active region show better carrier confinement in the GRINSCH diode. Thus, together with the large optical confinement, the GRINSCH diode could offer an unconventional path for the development of solid-state ultraviolet optoelectronic devices, mainly laser diodes of the future.

The ultraviolet light emitting devices, e.g., light emitting diodes (LEDs) and lasers, are critical in a variety of applications, including medical diagnostics, UV curing, optical non-line-of-sight communications, and water/air sterilization.¹ Those devices, made of aluminum gallium nitride (AlGaN) semiconductors which possess large and tunable bandgap from 3.4 to 6.1 eV and chemically robust, have a long lifetime and operationally stable, making them one of the top contenders to replace the current UV gas lasers and toxic, power consuming, and eco-unfriendly mercury-based UV lamps.^{1,2} As the operation wavelength requirements of the UV sources move towards shorter wavelengths, Al-rich AlGaN layers are indispensable in design and fabrication of the devices. However, Al-rich AlGaN layers suffer from a series of challenges in realizing highly crystalline material with efficient doping, which so far results in poor device performance characteristics.³ Deteriorated crystalline quality, resulting from the lattice-mismatched foreign substrate and short diffusion length of Al adatoms on a growing surface, is often observed during the deposition of Al-rich AlGaN epitaxial layers. The generated crystalline defects (dislocations) result in high leakage currents and suppress the radiative recombination efficiency in the active region which severely impact the device operation.^{4,5} Furthermore, high-conductivity p-type Al-rich AlGaN layers by Mg doping are difficult to obtain because of the low doping efficiency due to the high activation energy of the acceptor.^{6,7} Therefore, the threshold operating voltage and device series resistance of reported UV laser diodes are quite high. For instance, Yoshida et al. have demonstrated UV lasers at 336 and 342 nm which are the shortest wavelengths of laser diodes with high output power (>1 mW) to date.^{8,9} However, the operating voltages for both laser diodes surpass 25 V in the lasing mode due to poor hole injection efficiency.

Many approaches have been attempted to improve the conductivity of the layers by utilizing Mg doping in $\text{Al}_x\text{Ga}_{1-x}\text{N}/\text{Al}_y\text{Ga}_{1-y}\text{N}$ superlattices^{10, 11, 12, 13}, Mg delta doping^{14, 15, 16}, and tunnel-junction injection of nonequilibrium holes.^{17,18} In particular, a high sheet carrier density at the interface of the $\text{Al}_x\text{Ga}_{1-x}\text{N}/\text{Al}_y\text{Ga}_{1-y}\text{N}$ heterojunction was theoretically predicted and experimentally demonstrated.¹⁹ Two-dimensional (2D) electron or hole gas can be generated for high power transistor applications.^{19, 20, 21} Most importantly, polarization-induced three-dimensional (3D) electron and hole gases can be created by introducing a compositional AlGaN grading profile, instead of an abrupt AlGaN heterojunction.^{22,23,24,25} Such 3D free

1 electrons and holes usually originate from donor- and acceptor-like impurities or defects via
2 polarization-induced ionization process, and have been implemented in AlGaN-based planar UV emitters^{26,27,28}
3 without any intentional doping.²³
4
5
6

7 Compared to the AlGaN epitaxial thin-film layers, p-type AlGaN nanowires were recently found to have lower
8 resistivity owing to more efficient Mg incorporation and lower activation energy which are caused by the
9 reduced lattice strain imposed by surface dopants, compared to bulk dopants.^{29,30,31} This observation is
10 consistent with earlier discoveries that semiconductor nanowires often have higher doping efficiency than
11 thin-film layers, such as InN³², Si, and Ge nanowires.^{33,34,35,36,37} Furthermore, due to the efficient strain
12 relaxation associated with the large surface-to-volume ratio, nearly defect-free AlGaN nanowires can be grown
13 directly on many substrates.^{38,39} Hence, the development of new UV sources made of AlGaN nanowires have
14 been a field of high interest. In this context, polarization-induced doping together with the distinctly better
15 electrical conductivity of p-type Al-rich AlGaN nanowires has been suggested to address the material
16 challenges, e.g., high-density dislocations and low p-doping efficiency in the AlGaN layers. However, only a
17 few attempts have been made.^{40,41} In these efforts, nanowire structures were grown by molecular beam epitaxy
18 (MBE) under N-rich conditions, and the polarization-induced doping was realized by linearly grading the
19 structure from GaN to AlN and then from AlN to GaN. However, such direct grading from GaN to AlN
20 nanowires leads to polarization-induced hole doping due to the nature of N-polarity of the nanowires, forcing
21 those nanowires to start with p-type on a p-type substrate (e.g., p-Si). The nanowire-based devices with such a
22 “bottom p-type” structure raises several issues: (1) p-Si has a substantial valence band offset with p-GaN,
23 resulting in poor hole injection into the active region of the device; (2) a memory effect of Mg dopant could
24 deteriorate the performance of devices grown by both MBE and metalorganic chemical vapor deposition
25 (MOCVD); (3) p-type substrates have poor electrical performance than n-type. Furthermore, an amorphous
26 insulating SiN_x layer is often observed when nanowires were grown directly on Si,^{42,43} increasing the interfacial
27 resistance, thus requiring a higher device operating voltage.
28
29
30
31
32
33
34
35
36
37
38
39
40
41
42
43
44

45 Here, we design, grow, and characterize AlGaN nanowires on metal-coated n-Si substrates in the form of
46 graded-index separate confinement heterostructure (GRINSCH). A Ti/TaN metal-bilayer is deposited on n-Si
47 prior to the nanowire growth to avoid the formation of the insulating SiN_x layer.⁴⁴ The compositional gradient
48 of Al content along the growth direction is carefully designed and controlled. For comparison, nanowires with a
49 conventional p-i-n diode configuration are also prepared. Detailed optical and electrical studies of both
50 structures are carried out. We demonstrate the superior performance of GRINSCH diodes compared to the
51 conventional p-i-n counterparts. In the end, it is recognized that the GRINSCH diodes could offer a unique
52
53
54
55
56
57
58
59
60

structure for the realization of efficient UV emitters, and most importantly, their potentials in the implementation of UV laser diode owing to a better carrier and optical confinement,

Experimental Section

The nanowires studied in this work were grown by a Veeco GEN-930 plasma-assisted molecular beam epitaxy. Prior to the AlGa_xN nanowire growth, a ~20 nm TaN diffusion barrier was deposited on a (100) n-type Si substrate ($10^{-1} \Omega \cdot \text{cm}$) using atomic layer deposition (ALD) at 300 °C. A precursor was purged with Ar (200 sccm) and H₂ plasma (50 sccm) during the deposition, followed by a ~100 nm Ti layer deposited by an e-beam evaporator. Our previous study shows that by inserting a 20 nm TaN interlayer between a Ti pre-orienting layer and the Si substrate, we were able to improve carrier injection and nanowire uniformity.⁴⁴ Furthermore, this Ti/TaN metal-bilayer can also inhibit the Ti/Si interdiffusion, which can cause surface delamination during the nanowire nucleation at high growth temperatures. Such surface delamination leads to an extremely rough surface and causes a non-uniform growth of the nanowires (the height of nanowires varies in a range of ~100 nm).^{45,46} By inserting the TaN interlayer, the surface roughness of Ti/TaN metal-bilayer-coated Si can be as low as 1.6 nm, and thus the nanowires grown on top have high density and aligned well vertically with similar height, making the additional surface planarization process unnecessary.⁴⁴ After metal coating, the Ti/TaN/Si substrate was then outgassed in the MBE load lock at 200 °C for 1 hour (h) followed by outgassing in the buffer chamber at 600 °C for 2 h to remove moisture and molecular adsorption for subsequent growth. For the nanowire growth, first of all, Si-doped n-GaN seeds were initiated at a substrate temperature of 485 °C for 1 min to reduce Ga adatom desorption and increase the nucleation probability. The Ga beam equivalent pressure (BEP) was 6.0×10^{-8} Torr, the Si effusion cell was kept at 1180 °C, and the high-brightness nitrogen plasma was sustained using 350 W RF power and 1-sccm flow rate. In this condition, less than 3 nm of n-GaN was grown. The temperature was then raised to 630 °C to grow a bottom n-AlGa_xN layer. We estimated the nominal Al composition based on the ratio of the Al BEP to Ga BEP. The active region is composed of 10 stacked repetitions of alternating Al_xGa_{1-x}N quantum well(QW) with Al and Ga BEPs of 2.0×10^{-8} and 5.5×10^{-8} Torr, respectively, suggesting an approximately 20~25% of the Al-content in the QW and the Al_yGa_{1-y}N quantum barriers (Al and Ga BEPs of 2×10^{-8} and 3×10^{-8} Torr, hence $y > x$) with thicknesses of ~3 and ~6 nm, respectively, grown at 630 °C. After the growth of a p-AlGa_xN electron blocking layer (EBL) at 600 °C, p-AlGa_xN layers were then grown at 610 °C with Al and Ga BEPs of 2×10^{-8} and 3×10^{-8} Torr, respectively, while the Mg cell temperature was kept at 360 °C with the same nitrogen plasma condition. An additional highly doped p-GaN contact layer was grown by increasing the Mg cell temperature to 380 °C and reducing the growth temperature to 580 °C. All layers were grown under N-rich conditions. The Al_zGa_{1-z}N graded layers were grown by linearly changing the temperature of the Ga effusion cell on the basis of the beam-flux

1 calibration. The Ga flux increased linearly from 2×10^{-8} to 4.5×10^{-8} Torr for the bottom grading layer and
2 decreased from 4.5×10^{-8} to 2×10^{-8} Torr for the top grading layer. At the same time, the Al flux was
3 maintained at 2×10^{-8} Torr. For the comparison of GRINSCH and conventional diodes, the same procedure and
4 growth conditions were applied including the same heater and cell temperatures at each stage of the growth.
5
6
7

8
9 The devices were fabricated using standard UV contact-lithography techniques.⁴⁷ Immediately after the
10 lithography, the sample was dipped in 20% HF to remove surface oxidation before Ni/Au (5 nm/5 nm)
11 blanket-evaporation and annealed in 1 min at 600 °C using rapid thermal processing after evaporation. Further
12 evaporation of Ni/Au (10 nm/200 nm) was carried out to define contact-fingers and probe-pads using
13 photoresist and UV contact lithography. Finally, the Si back-surface was etched away by 200 nm using
14 inductively-coupled plasma reactive-ion etching (ICP RIE) in preparation for depositing Ti/Au (10 nm/150 nm)
15 n-contacts. Temperature-dependent photoluminescence (PL) measurements were performed, and the samples
16 were excited with a third harmonic mode (~260 nm) of mode-locked Ti: sapphire oscillator operating at ~ 780
17 nm. The PL signal was collected by using a UV objective and then measured by an OceanOptics QEPro
18 spectrometer. Electroluminescent (EL) signal was also measured, and the current was injected by using a
19 Keithley source 2450C operating in continuous mode at different injection currents. Scanning electron
20 microscopy (SEM) and scanning transmission electron microscopy (STEM) were used to investigate the quality
21 and structure of the nanowires. SEM images were taken using Zeiss Supra 40. A Thermofisher USA (former
22 FEI) Titan Themis Z microscope was utilized for STEM characterization. The microscope was operated at the
23 accelerating voltage of 300 kV. Atomic-number sensitive (Z-contrast) STEM was realized by acquiring the data
24 with high-angle annular dark-field (HAADF) detector. The equilibrium energy band diagram and the carrier
25 distribution profiles (both electrons and holes) across the entire structure were simulated and analyzed using the
26 commercially available software package Crosslight APSYS program.^{48,49,50} The energy band diagram of the
27 structure was obtained by self-consistently solving Poisson's equation under thermal equilibrium condition,
28 meanwhile taking into account of the existence of strong spontaneous and piezoelectric polarization charges in the
29 AlGaIn alloys. For valence band, the 6×6 *k*·*p* method was adopted, taking into account the non-parabolic nature
30 of the energy bands. The optical mode profile and optical confinement were computed by numerical solution
31 finite-difference-time-domain (FDTD) software package.
32
33
34
35
36
37
38
39
40
41
42
43
44
45
46
47
48
49

50 Results and Discussion

51 Structural design and characterization

Here, we have demonstrated two different types of AlGaIn nanowire diode structures: compositionally graded AlGaIn layers embedded in nanowires (denoted as GRINSCH diode) and conventional p-i-n nanowires. The sequence of layers in both diodes is schematically illustrated in Figure 1 (a) and (b), respectively. The GRINSCH diode consists of a 250 nm n-Al_{0.5}Ga_{0.5}N layer, a 50 nm Si-doped graded Al_zGa_{1-z}N layer with decreasing the Al composition from 50% to 30% towards the growth direction, followed by 10 pairs Al_xGa_{1-x}N/Al_yGa_{1-y}N multiple quantum wells (MQWs). This is followed by a ~8 nm high Al-content Mg-doped AlGaIn electron blocking layer (EBL), and a 50 nm Mg-doped reversed graded Al_xGa_{1-x}N layer with increasing Al content from 30% to 50%. Finally, a 40 nm Mg-doped Al_{0.4}Ga_{0.6}N layer and a very thin (~3 nm) heavily doped p-GaN contact layer were grown. The design of the conventional p-i-n diode is similar to the GRINSCH diode but the bottom- and top-graded AlGaIn layers which were replaced by an AlGaIn layer with 40% of Al content.

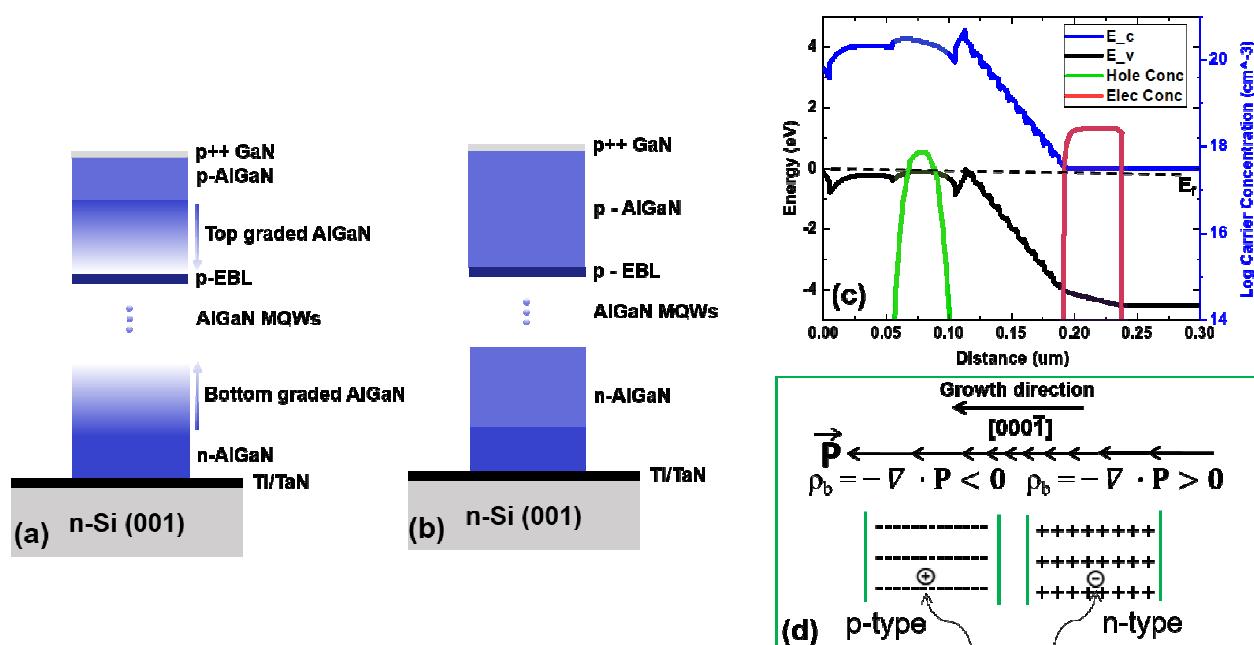


Figure 1. Schematic structures of the (a) GRINSCH diode and (b) conventional p-i-n diode. (c) Simulated energy band diagram of the GRINSCH diode structure with 10 MQWs under thermal equilibrium and electron and hole concentrations in compositionally graded AlGaIn layers. (d) Schematic illustration of polarization-induced n-type (positive polarization charge at bottom grading AlGaIn layer) and polarization-induced p-type (negative charge at top grading AlGaIn layer) in the GRINSCH diode along the [000 $\bar{1}$] crystallographic direction (N-polarity). It also shows that a continuous change in the polarization vector in the growth direction creates polarization charge fields.

The energy band diagram (under thermal equilibrium) and the profile of the polarization-induced electron and hole distribution in the GRINSCH diode are included in Figure 1(c). Typically, the MBE-grown nitride

1 nanowires possess N-polarity due to the N-rich condition. Thus, a compositional gradient of decreasing
2 Al-content from 50 % to 30 % along the growth direction $[000\bar{1}]$ creates a positive polarization charge field as the
3 magnitude of the polarization field varies slowly, resulting in a fixed 3D space bound charge $\rho_b = -\nabla \cdot \mathbf{P}$ (non-zero
4 gradient of the polarization vector \mathbf{P}).²⁶ These positive space charges attract free electrons from surrounding
5 materials (e.g. surface states, defects, dopants) and consequently a 3D electron gas reservoir is formed, realizing
6 an n-type conductivity of the graded AlGa_N layer (as shown in Figure 1(d) right). Similarly, in the symmetric
7 part (p-AlGa_N layer) of the graded structure where the Al-content is increased linearly from 30 % to 50 % after
8 the active region growth, a constant negative polarization charge across the graded region is formed. Then, an
9 equivalent amount of free holes are induced, spreading over the graded AlGa_N layer, by the polarization field to
10 neutralize these negative charges, giving rise to a mobile 3D hole gas (Figure 1(d) left), and thus, p-type doping
11 is realized.^{27,28} Such polarization-induced doping technique is feasible to directly control the density of free
12 electron/hole charges by varying either the Al-content and/or the AlGa_N thickness.²⁷ Furthermore, a p-n
13 junction can be realized by simply grading AlGa_N layers without using conventional impurity doping.^{22,28}
14 Moreover, the realization of polarization doping does not freeze out at low temperature due to field ionization,
15 so the electron and hole concentration can be enhanced, independent of temperature.²⁶ These advantages of
16 polarization doping offer a unique solution to effectively increase both the carrier concentration and mobility by
17 reducing ionized impurity scattering.^{26,28} Most importantly, the inclusion of additional impurities (donors or
18 acceptors) along with polarization doping could further enhance the electrical conductivity of n- and p-type
19 AlGa_N layers.^{23,24,51}

20
21
22
23
24
25
26
27
28
29
30
31
32
33
34
35 The calculated band diagram indicates the formation of a p-n junction due to polarization-induced p- and n-type
36 doping of the AlGa_N graded layers on either side of the active region.^{22,23} Shown in the same figure (Figure
37 1(c)) are also the concentration of holes and electrons induced by polarization doping. It should be stressed that
38 such a high concentration of electrons and holes ($1 \sim 2 \times 10^{18} \text{ cm}^{-3}$) in the p-n junction is obtained without the
39 utilization of intentional impurities and dopants. This doping level in both sides of the junction assumes the
40 existence of a sufficient amount of acceptor-like or donor-like impurities or defects (including surface charges)
41 in either side of the junction, which can be ionized by polarization.^{16,24,26,28} In reality, such impurities or defects
42 may occur naturally during the growth process or may be introduced intentionally by incorporating n-type
43 dopants (Si) in the first AlGa_N compositionally graded layer and p-type dopants (Be or Mg) in the second
44 AlGa_N compositionally graded layer.²⁶ The effectiveness of this polarization doping (or polarization-enhanced
45 doping) technique has been previously demonstrated in planar UVLEDs.^{23,26,28}

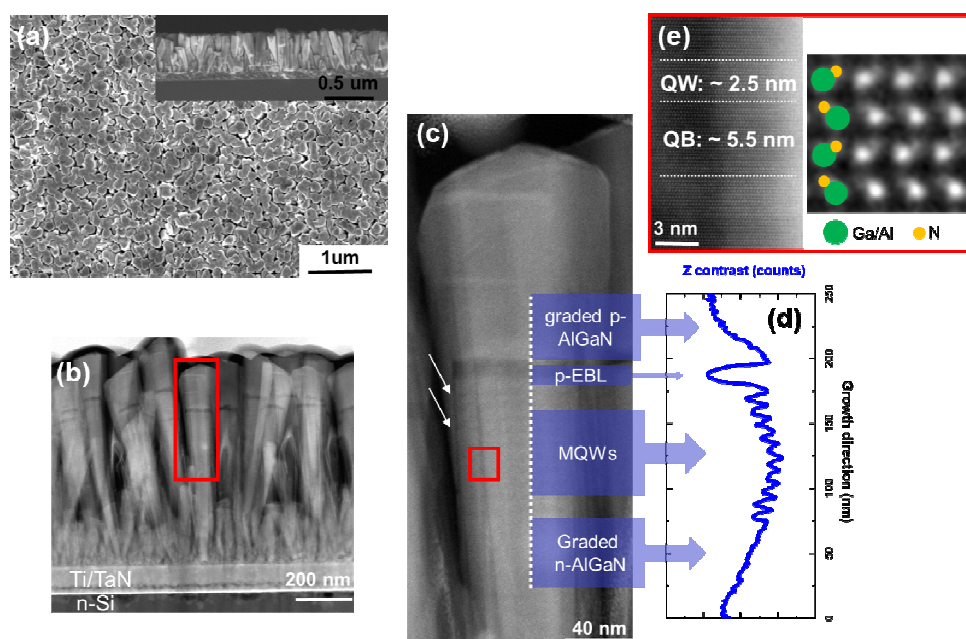


Figure 2. (a) Top-view and cross-sectional (inset) SEM images of GRINSCH diode. (b) Cross-sectional HADDF-STEM image of GRINSCH diode. (c) Enlarged STEM image marked in red rectangular in (b), showing a single nanowire. The white arrows mark the shell of the nanowire. (d) Z-contrast profile of the dashed line marked in (c), the darker area indicates higher Al content. (e) Atomic resolution STEM image of the quantum well and barrier (red square marked in (c)) with the atomic arrangement of Al/Ga and nitrogen atoms along the growth direction schematically.

Illustrated in Figure 2 (a) is the SEM image of the GRINSCH nanowires. The nanowires are vertically aligned on the Ti/TaN-coated Si substrate and exhibit relatively uniform height and size distribution (the lateral size is in the range of 120-150 nm and a height of ~ 750 nm) which is further confirmed by the cross-sectional STEM image (Figure 2(b)). No interface delamination is observed between the Ti/TaN metal-bilayer and Si substrate, resulting in a relatively uniform nanowire distribution across the entire wafer. The filling factor is estimated to be 96%, representing extremely compact and high-density nanowires. The nearly coalesced nanowires at the top surface provide a simplified fabrication process that we can deposit metal pads directly without using any filling materials to planarize the nanowires.⁴⁵ It has to be stressed that a surface planarization step by filling the gaps between nanowires using a polymer (e.g., parylene or polyimide) before depositing metal pads is commonly implemented in fabricating nanowire-based devices.^{45,46} However, this planarization process may oxidize the top p-GaN layer during the etch-back procedure which may cause serious damage to the device during the operation. Figure 2(c) shows an enlarged image of the GRINSCH nanowire with the clear observation the formation Al-rich shell (pointed by the white arrows). Such a spontaneously formed large bandgap AlGaN shell on the sidewall of each nanowire suppress the non-radiative surface recombination and could act as a

self-passivated layer to reduce surface states for the visible/UV LEDs and lasers.^{52,53} The Z-contrast profile shows the integrity of GRINSCH diode nanowire including both graded AlGaIn layers, MQWs, and the other part of the structure. Due to the low Al-content difference (only 10%), the color contrast between the QW and barrier layer is hardly noticeable. The nanowires in the conventional p-i-n diode exhibit similar structural properties. Nanowires in both diodes were grown along the *c*-axis and possess N-polarity which is commonly observed in the MBE-grown nanowires, as confirmed in the atomic resolution image of the quantum well and barrier in Figure 2(e).

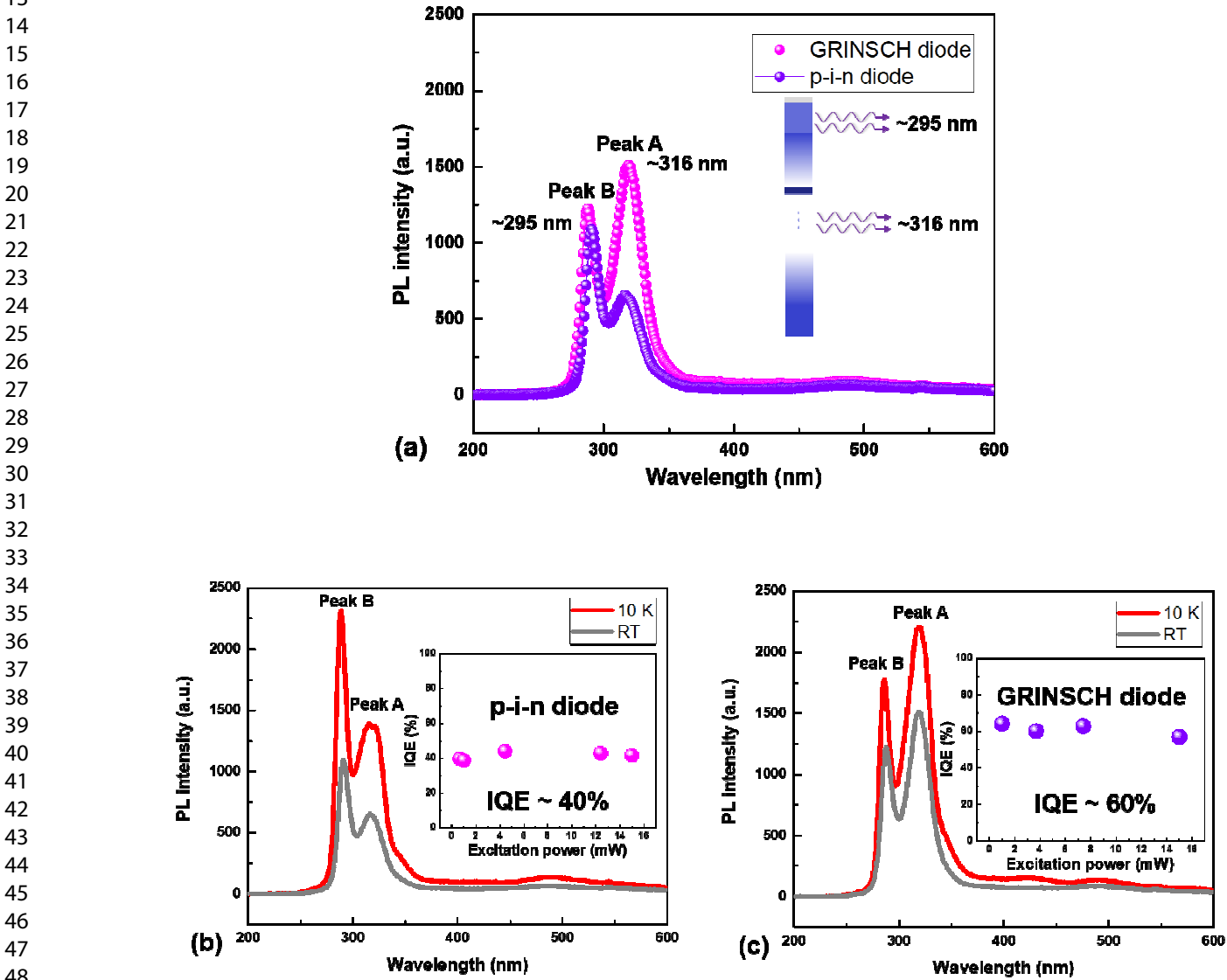


Figure 3. (a) PL spectra of the GRINSCH diode and p-i-n diode at room temperature (RT). PL spectra measured under an excitation power of ~4 mW at RT and 15 K for (b) GRINSCH and (c) p-i-n diode. The inset shows the internal quantum efficiency versus excitation power.

Photoluminescence and electroluminescence characterization

Temperature-dependent PL measurements of the investigated GRINSCH and p-i-n diode were performed. Shown in Figure 3 (a), the nanowires heterostructure exhibits strong emission at ~ 316 nm (Peak A) with FWHM values of 19.8 and 19.1 nm for the GRINSCH and p-i-n diode, respectively. A slight broadening of the PL spectrum of the GRINSCH diode could be attributed to the graded AlGaIn layer where it may have compositional inhomogeneities along the grading direction. These values of the FWHM are similar to the reported AlGaIn-based nanowire UV emitters^{17,41,44,52}, suggesting the good quality of the nanowires. Emission from the higher Al-content AlGaIn nanowire segment (mainly from the top p-AlGaIn layer) can also be observed (Peak B: ~ 295 nm). The ratio of Peak A and Peak B is 1.24 and 0.58 for the GRINSCH- and p-i-n-diode, respectively. The high-luminescence intensity of the GRINSCH diode from the active region could be directly related to the significantly improved carrier flow into quantum wells assisted by the graded AlGaIn layers and thus higher recombination in the active region. Furthermore, the internal quantum efficiency (IQE) is also estimated by dividing the integrated PL intensity at RT with that measured at 10 K, as shown in Figure 3(b) and 3(c). The IQE of the GRINSCH diode is nearly 50% higher than the p-i-n diode over a large range of excitation power. Earlier studies in traditional compound semiconductors, such as GaAs and InP-based GRINSCH laser diodes show much lower optical and electrical pumping thresholds compared with abrupt heterojunctions.^{54,55} This is mainly attributed to the additional photo-generated carriers in the grading layer.^{56,57} These carriers flow into the active region, creating higher luminance performance similar to the observation of a higher intensity of Peak B in the AlGaIn GRINSCH diode.

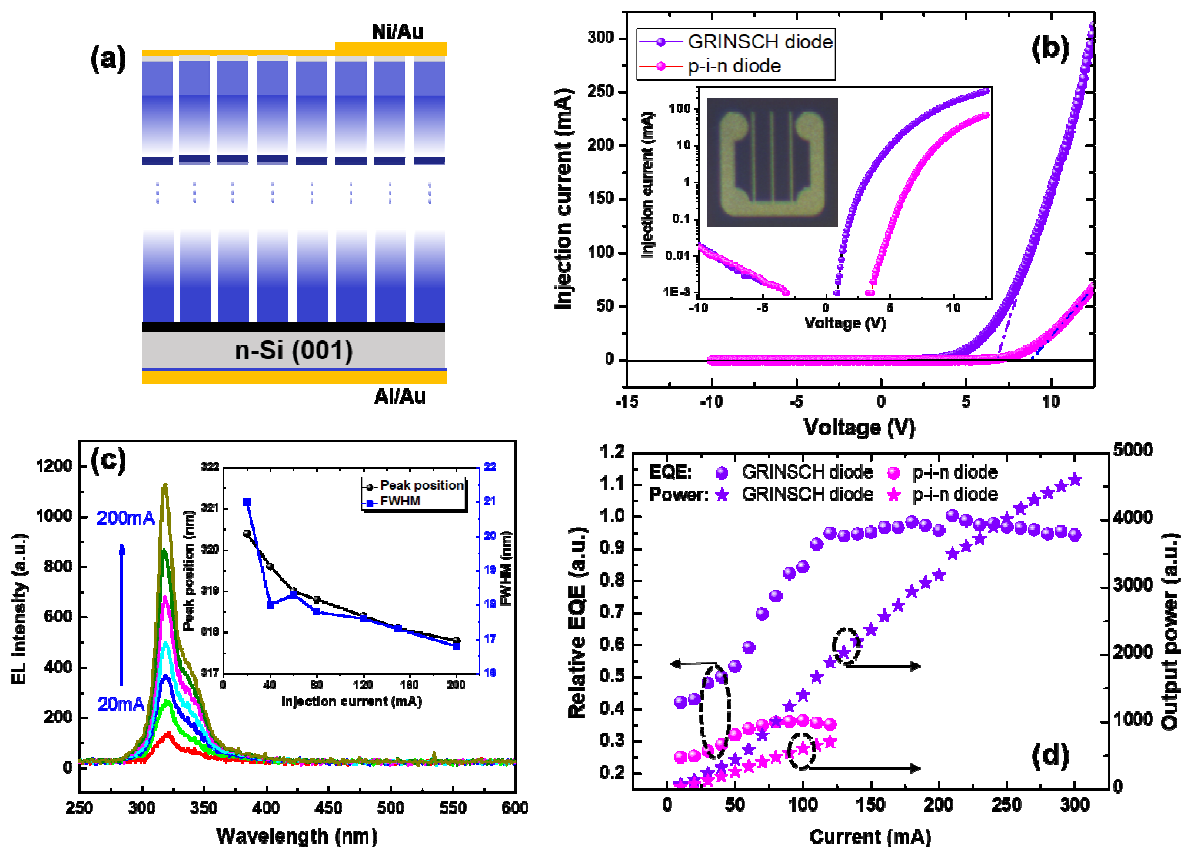


Figure 4 (a) 2D schematic illustration of the fabricated AlGaIn nanowire diode on Ti/TaN-coated Si substrate. (b) Current-voltage characteristic of the GRINSCH and p-i-n diode. The inset shows the semilog plots of the I-V curves and an optical image of a GRINSCH diode. (c) EL spectra of the GRINSCH diode varying injection current from 20 to 200 mA. The inset shows the FWHM and peak position of the EL spectra under the same range of injection current. (d) Measured output power and relative EQE of the GRINSCH and p-i-n diodes under the biasing current from 10 to 300 mA. Due to the high resistivity of AlGaIn nanowires in the p-i-n diode, the maximum injection current can only reach 120 mA.

The light-current-voltage (L-I-V) characteristics of both GRINSCH and p-i-n diodes are measured under different injection current under continuous-wave (CW) biasing conditions. Figure 4(a) depicts the fabricated device. Because of the nearly coalesced (filling factor $\sim 96\%$) top surface of the nanowires (as shown in the Figure 2(a)), we simply employed a standard photolithography procedure to define the current spreading layer for the hole injection.⁴⁷ The Al/Au and Ni/Au metal stack was deposited directly to the n-Si substrate and p-GaN layer to form an ohmic contact, respectively. The device mesa size is $500 \times 500 \mu\text{m}^2$ for both diodes. From the I-V characteristics, it can be seen that both diodes show a usual rectifying behavior. Noted in Figure 4(b), the turn-on voltage is around 6.5 V for the GRINSCH diode, whereas it is 8.9 V for the p-i-n diode. A similar leakage current is observed in both diodes, as shown in the inset of Figure 4(b). Most importantly, the

series resistance, which is extracted from the slope of the I-V characteristic in the linear region between 10 and 12.5 V for both diodes, is as low as $16.7\ \Omega$ in the GRINSCH diode, nearly four times smaller than the one in the p-i-n diode ($\sim 58.1\ \Omega$). This significant reduction of the series resistance is attributed to the pronounced resistivity reduction of the body of the AlGaIn nanowires owing to the effective polarization-induced n- and p-doping by incorporating the compositionally graded AlGaIn layers adjacent to the active region. In the GRINSCH configuration, in addition to the thermally activated electrons and holes from the Si-donors and Mg-acceptors, polarization-induced doping also provides ionizing donor and acceptor dopants using the intrinsic built-in electronic polarization in the AlGaIn crystals, as confirmed by its band diagram (Figure 1(c)).²⁶ Because of the major improvement in the n- and p-type electrical conductivity, a lower turn-on voltage and smaller sheet resistance are expected, which is similar to the previous reports in the planar UVLED structures.^{23,26}

Shown in Figure 4(c) is the EL spectra measured under various injection currents under CW biasing condition for GRINSCH diode. A relatively narrow emission peak centered at 318 nm was measured. The spectral line width (full width at half-maximum: FWHM) is ~ 20 nm at the 20 mA and reduced to ~ 17 nm when the current is increased up to 200 mA. This relatively small value of FWHM is close to the one reported in UVLEDs incorporating planar AlGaIn MQWs in similar peak emission regime.^{18,58,59} A blue shift of ~ 3 nm in the emission wavelength was measured with increasing injection current, indicating small quantum-confined Stark effect. No defect-related emission in the visible spectral range was observed. The output power of nanowire diodes was measured directly on the wafer without any packaging under CW biasing. Shown in Figure 4(d), the output power continuously rises as the injection current increases for the GRINSCH diode. Noticeably, the GRINSCH diodes sustain the injection current as high as 320 mA compared to the conventional p-i-n diode (120 mA) for the device size $500 \times 500\ \mu\text{m}^2$. Such drastically improved electrical injection and output power of the GRINSCH diode is attributed to the significantly enhanced electron/hole transport and injection into the active region because of the polarization induced doping. The relative external quantum efficiency (EQE), is measured by taking the ratio of the number of emitted photons over the number of injected electrons. EQEs of both diodes versus injection current under CW operation are presented in Figure 4(d). For the conventional p-i-n diode, the device operation saturated immediately at low current injection due to its low conductivity of the nanowires themselves, resulting in low output power and low EQE performance. Nevertheless, in GRINSCH diode, EQE increases almost linearly with the increase in injection current up to 120 mA. It then plateaus up to 320 mA. We didn't observe any significant efficiency droop as observed in the conventional p-i-n diode. Normally, the severe efficiency droop has been commonly measured in planar AlGaIn-based LED devices.^{58,59} The underlying mechanism for this droop may include Auger recombination and electron overflow

1 at high injection current.³ Such droop was also observed in our previous study where the AlGa_N nanowires
2 were grown directly on Si substrates.⁶⁰ It is reasonable to claim that NWs grown on Ti/TaN-coated Si substrate
3 have better thermal conductivity, which helps to dissipate heat efficiently at high injection current compared to
4 the ones grown on conventional Si or sapphire substrates. Therefore, the nanowires grown on metal substrates
5 or on metal-coated substrates are desirable for high-current injection light-emitting devices. It is expected that
6 with further optimization of the design and epitaxy process of AlGa_N nanowires, both the turn-on voltage and
7 resistance of nanowire diodes in the GRINSCH configuration can be further reduced.
8
9
10
11
12
13

14 **A step toward UV laser diode implementation**

15
16
17

18 Previously, such a GRINSCH diode configuration has been implemented in conventional III-V
19 compounds-based (e.g., GaAs, InP) devices, particularly in laser diodes, by virtue of the simultaneous
20 improvement of carrier injection and vertical optical mode confinement, as pioneered by the Kazarinov et al.
21 and Tsang et al.^{54,55} GaAs and InP-based GRINSCH laser diodes, with either linear or parabolic shape of the
22 graded-index profile, have achieved extremely low threshold currents and thus have been commercialized in
23 semiconductor industry.^{56,57} Recently, a GRINSCH-based InGa_N laser diode was also demonstrated, showing
24 very promising low threshold current density of 3.5 kA/cm², compared with the classical step-index structure.⁶¹
25 However, for the aforementioned devices, the advantage of polarization doping technique has not been taken
26 into account because both n- and p-doping are easily achieved in the InGa_N layers. For the realization of
27 electrically pumped AlGa_N-based laser diode, we face a tremendous challenge to obtain a conductive p-type
28 Al-rich AlGa_N layer because of the high ionization energies of Mg-acceptors. Thus, any breakthrough in the
29 development of electrically-injected UV semiconductor laser diode will highly depend on the capability to
30 efficiently p-dope high Al content AlGa_N layers. Therefore, a semiconductor UV laser diode design, which can
31 take advantage of the polarization-enhanced p-type doping via compositional gradient of Al-content in the
32 AlGa_N layers while achieving better carrier and optical mode confinement is a structure having the GRINSCH
33 configuration.^{62,63}
34
35
36
37
38
39
40
41
42
43
44
45
46
47
48
49
50
51
52
53
54
55
56
57
58
59
60

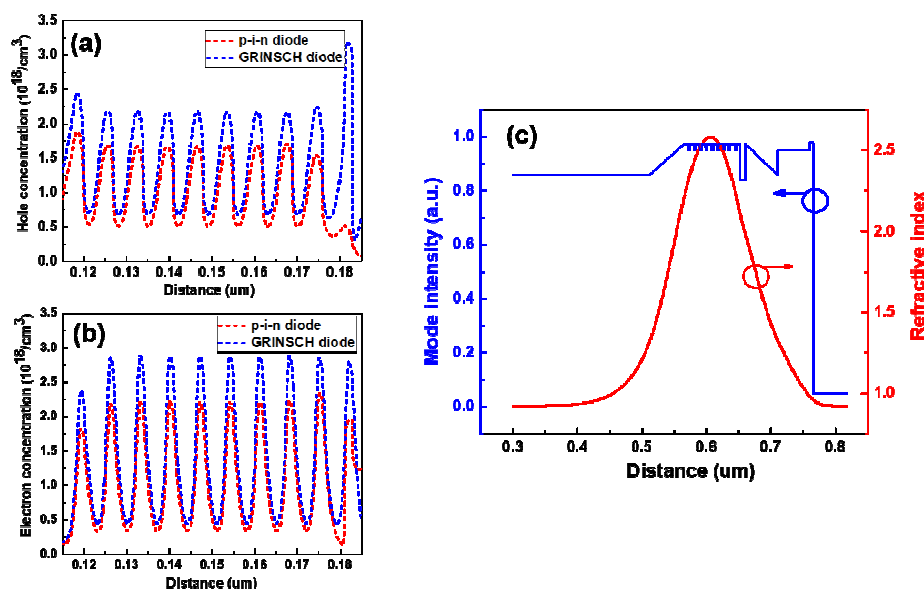


Figure 5 (a) Hole and (b) electron concentrations for the GRINSCH diode (blue dash line) and the conventional diode (red dash line) at 200 mA; (c) Vertical profile of the index of refraction and the optical mode profile for the GRINSCH diode.

Figure 5 (a) and (b) show the calculated hole and electron concentrations under a current injection of 200 mA for both diode, respectively. Significant increases in the hole and electron concentrations by 81.1% and 29.5%, respectively, can be expected in the GRINSCH diode compared with the traditional p-i-n one. Such improvement is attributed to better carrier confinement and possibly high current injection efficiency with the aid of the polarization-induced doping due to compositionally graded AlGa_xN layers on either side of the active region. Furthermore, the near-field optical model profile and the vertical profile of the index refraction in the GRINSCH diode are depicted in Figure 5 (c), computed by the FDTD numerical simulation. Refractive indices were extracted from Brunner et al.⁶⁴ for the AlGa_xN and graded Al_xGa_{1-x}N layers at the targeted emission wavelength of 315 nm. The optical mode is well confined by the graded AlGa_xN layers, with an optical confinement factor, Γ , in the active region of the device of 17.9 %. Such a large optical confinement value could provide the confidence of the suitable laser structure by adopting GRINSCH configuration, as most of the reported AlGa_xN MQW-based lasers has only 1~3% optical confinement.^{8,9} Admittedly, further optimization of the active region, such as the number of QWs as well as the thickness of each QW and QB layer, is also critical to achieve single mode lasing with the reduced internal material loss.⁶³

The above results show a feasible approach to realize UV laser diode using the AlGa_xN-based GRINSCH configuration, especially the demonstration of efficient high current injection and reduced series resistance, we still face challenges in fabricating such nanowire-based laser diodes. On the basis of the extreme surface

sensitivity due to large surface to volume of nanowires and the fact that difficulty in fabricating high reflectivity mirrors for lasing, extensive efforts are required to overcome these obstacles. Recently, InGaN nanowire structures, including green and red edge emitting lasers have been reported,^{65,66} thus the present effort paves the way towards the realization of UV laser diode based on dislocation-free nanowires.

Conclusion

In this context, a novel AlGaIn-nanowires-based diode by adopting GRINSCH configuration in which we embedded the active region between two compositionally graded AlGaIn layers was proposed and characterized. We demonstrated that the AlGaIn-based GRINSCH diode, with the nearly coalesced surface (filling factor > 96%), possesses encouraging electrical and optical performance compared to the conventional p-i-n diode. A lower turn-on voltage of 6.5 V and significant reduction of the series resistance by almost four times in the GRINSCH diode are achieved. Such improved electrical characteristics show strong evidence of the effectiveness of polarization-induced n- and p-doping in the compositionally graded AlGaIn layers which eventually enhance the carrier injection efficiency. The numerical analysis indicates a higher electron and hole concentrations in the active region and large optical confinement for the GRINSCH diode. Therefore, the proposed GRINSCH diode brings us one step forward to the eventual demonstration of AlGaIn-based laser diodes.

AUTHOR INFORMATION

Corresponding Authors

[#]haiding.sun@kaust.edu.sa, ^{##}boon.ooi@kaust.edu.sa, ^{###}xiaohang.li@kaust.edu.sa

Notes

The authors declare no competing financial interest.

Acknowledgments

We acknowledge the financial support from King Abdullah University of Science and Technology (KAUST) baseline funding, BAS/1/1614-01-01, BAS/1/1664-01-01, BAS/1/1376-01-01 and KAUST CRG URF/1/3437-01-01. Also, BSO, TKN, RCS, MKS, CZ, JWM, and DP gratefully acknowledge funding support from King Abdulaziz City for Science and Technology, grant no. KACST TIC R2-FP-008 and KAUST MBE equipment funding, C/M-20000-12-001-77. The work at University of Houston was supported by King

Abdullah University of Science and Technology (KAUST) (contract #: OSR-2017-CRG6-3437.02). JHR also acknowledge partial financial support from the Texas Center for Superconductivity at the University of Houston (TcSUH).

Reference

- ¹ Khan, A.; Balakrishnan, K.; Katona, T. Ultraviolet light-emitting diodes based on group three nitrides Nat. Photonics **2008**, 2, 77– 84
- ² Li, X.; Xie, H.; Ryou, J. H.; Ponce, F. A.; Detchprohm, T.; Dupuis, R. D. Onset of surface stimulated emission at 260 nm from AlGaN multiple quantum wells Appl. Phys. Lett. **2015**, 107, 241109
- ³ Kneissl, M.; Rass, J. III-Nitride Ultraviolet Emitters Springer: Switzerland **2016**, Chapter 1, Page 1-25
- ⁴ Kamiyama, S.; Iwaya, M.; Hayashi, N.; Takeuchi, T.; Amano, H.; Akasaki, I.; Watanabe, S.; Kaneko, Y.; Yamada, N. Low-temperature-deposited AlGaN interlayer for improvement of AlGaN/GaN heterostructure J. Cryst. Growth **2001**, 223, 83–91
- ⁵ Park, J. H.; Kim, D. Y.; Schubert, E. F.; Cho, J.; Kim, J. K. Fundamental limitations of wide-bandgap semiconductors for light-emitting diodes ACS Energy Lett. **2018**, 3, 655–662
- ⁶ Taniyasu, Y.; Kasu, M.; Makimoto, T. An aluminium nitride light-emitting diode with a wavelength of 210 nanometres Nature **2006**, 441, 325–328
- ⁷ Nakarmi, M. L.; Nepal, N.; Lin, J. Y.; Jiang, H. X. Photoluminescence studies of impurity transitions in Mg-doped AlGaN alloys Appl. Phys. Lett. **2009**, 94, 091903
- ⁸ Yoshida, H.; Yamashita, Y.; Kuwabara, M.; Kan, H. A 342-nm ultraviolet AlGaN multiple-quantum-well laser diode Nature Photon. **2008**, 2, 551.
- ⁹ Yoshida, H.; Yamashita, Y.; Kuwabara, M.; Kan, H. Demonstration of an ultraviolet 336 nm AlGaN multiple-quantum-well laser diode Appl. Phys. Lett. **2008**, 93, 241106
- ¹⁰ Ebata, K.; Nishinaka, J.; Taniyasu, Y.; Kumakura, K. High hole concentration in Mg-doped AlN/AlGaN superlattices with high Al content Jpn. J. Appl. Phys. **2018**, 57, 04FH09
- ¹¹ Cheng, B.; Choi, S.; Northrup, J. E.; Yang, Z.; Knollenberg, C.; Teepe, M.; Wunderer, T.; Chua, C. L.; Johnson, N. M. Enhanced vertical and lateral hole transport in high aluminum-containing AlGaN for deep ultraviolet light emitters Appl. Phys. Lett. **2013**, 102, 231106
- ¹² Martens, M.; Kuhn, C.; Ziffer, E.; Simoneit, T.; Kueller, V.; Knauer, A.; Rass, J.; Wernicke, T.; Einfeldt, S.; Weyers, M.; Kneissl, M. Low absorption loss p-AlGaN superlattice cladding layer for current-injection deep ultraviolet laser diodes Appl. Phys. Lett. **2016**, 108, 151108

13 Tahtamouni, T. M. A.; Lin, J. Y.; Jiang, H. X. Effects of Mg-doped AlN/AlGa_N superlattices on properties of p-GaN contact layer and performance of deep ultraviolet light emitting diodes AIP Adv. **2014**, 4, 047122

14 Wang, X.; Wang, W.; Wang, J.; Wu, H.; Liu, C. Experimental evidences for reducing Mg activation energy in high Al-content AlGa_N alloy by MgGa δ doping in (AlN)_m/(Ga_N)_n superlattice Sci. Rep. **2017**, 7, 44223

15 Chen, Y.; Wu, H.; Han, E.; Yue, G.; Chen, Z.; Wu, Z.; Wang, G.; Jiang, H. High hole concentration in p-type AlGa_N by indium-surfactant-assisted Mg-delta doping Appl. Phys. Lett. **2015**, 106, 162102

16 Liang, Y. H.;Towe, E. Heavy Mg-doping of (Al,Ga)N films for potential applications in deep ultraviolet light-emitting structures J. Appl. Phys. **2018**, 123, 095303

17 Sadaf, S. M.; Zhao, S.; Wu, Y.; Ra, Y.-H.; Liu, X.; Vanka, S.; Mi, Z. An AlGa_N core-shell tunnel junction nanowire light-emitting diode operating in the ultraviolet-C band Nano Lett. **2017**, 17, 1212-1218

18 Zhang, Y.; Krishnamoorthy, S.; Johnson, J. M.; Akyol, F.; Allerman, A.; Moseley, M. W.; Armstrong, A.; Hwang, J.; Rajan, S. Interband tunneling for hole injection in III-nitride ultraviolet emitters Appl. Phys. Lett. **2015**, 106, 141103

19Wood, C.; Jena, D. Polarization Effects in Semiconductors: From Ab Initio Theory to Device Applications Springer Science & Business Media **2007** Chapter 4, Page 161-216

20 Fang, Y.; Feng, Z.; Yin, J.; Zhou, X.; Wang, Y.; Gu, G.; Song, X.; Lv, Y.; Li, C.; Cai, S. AlGa_N/Ga_N Polarization-doped field-effect transistors with graded heterostructure IEEE Trans. Electron Devices **2014**, 61, 4084-4089

21 Wang, W.; Shervin, S.; Oh, S. K.; Chen, J.; Huai, Y.; Pouladi, S.; Kim, H.; Lee, S.-N.; Ryou, J.-H. Flexible AlGaInN/GaN heterostructures for high-hole-mobility transistors IEEE Electron Device Lett. **2017**, 38, 1086-1089

22 Sun, H.; Pecora, E. F.; Woodward, J.; Smith, D. J.; Dal Negro, L.; Moustakas, T. D. Effect of indium in Al_{0.65}Ga_{0.35}N/Al_{0.8}Ga_{0.2}N MQWs for the development of deep-UV laser structures in the form of graded index separate confinement heterostructure (GRINSCH) Phys. Status Solidi A **2016**, 213, 1165-1169

23 Sun, H.; Moustakas, T. D. UV emitters based on an AlGa_N p-n junction in the form of graded-index separate confinement heterostructure Appl. Phys. Exp. **2014**, 7, 12104.

24 Li, S.; Zhang, T.; Wu, J.; Yang, Y.; Wang, Z.; Wu, Z.; Chen, Z.; Jiang, Y. Polarization induced hole doping in graded Al_xGa_{1-x}N (x= 0.7~1) layer grown by molecular beam epitaxy Appl. Phys. Lett. **2013**, 102, 062108

25 Armstrong, A. M.; Allerman, A. A. Polarization-induced electrical conductivity in ultra-wide band gap AlGa_N alloys Appl. Phys. Lett. **2016**, 109, 222101

26 Simon, J.; Protasenko, V.; Lian, C.; Xing, H.; Jena, D. Polarization-induced hole doping in wide-band-gap uniaxial semiconductor heterostructures Sci. **2010**, 327, 60–64

- ²⁷ Lytvyn, P. M.; Kuchuk, A. V.; Mazur, Y. I.; Li, C.; Ware, M. E.; Wang, Z. M.; Kladko, V. P.; Belyaev, A. E.; Salamo, G. J. Polarization effects in graded AlGaIn nanolayers revealed by current-sensing and Kelvin probe microscopy ACS Appl. Mater. Interfaces **2018**, 10, 6755-6763
- ²⁸ Li, S.; Ware, M.; Wu, J.; Minor, P.; Wang, Z.; Wu, Z.; Jiang, Y.; Salamo, G. J. Polarization induced pn-junction without dopant in graded AlGaIn coherently strained on GaN Appl. Phys. Lett. **2012**, 101, 122103
- ²⁹ Tran, N.; Le, B.; Zhao, S.; Mi, Z. On the mechanism of highly efficient p-type conduction of Mg-doped ultra-wide-bandgap AlN nanostructures Appl. Phys. Lett. **2017**, 110, 032102
- ³⁰ Zhao, S.; Woo, S. Y.; Bugnet, M.; Liu, X.; Kang, J.; Botton, G. A.; Mi, Z. Three-dimensional quantum confinement of charge carriers in self-organized AlGaIn nanowires: A viable route to electrically injected deep ultraviolet lasers Nano Lett. **2015**, 15, 7801–7807
- ³¹ Zhao, S.; Connie, A. T.; Dastjerdi, M. H.; Kong, X. H.; Wang, Q.; Djavid, M.; Sadaf, S.; Liu, X. D.; Shih, I.; Guo, H.; Mi, Z. Aluminum nitride nanowire light emitting diodes: Breaking the fundamental bottleneck of deep ultraviolet light sources Sci. Rep. **2015**, 5, 8332
- ³² Zhao, S.; Le, B.; Liu, D.; Liu, X.D.; Kibria, M.; Szkopek, T.; Guo, H.; Mi, Z. p-Type InN nanowires Nano Lett. **2013**, 13, 5509–5513
- ³³ Perea, D. E.; Hemesath, E. R.; Schwalbach, E. J.; Lensch-Falk, J. L.; Voorhees, P. W.; Lauhon, L. J. Direct measurement of dopant distribution in an individual vapour–liquid–solid nanowire Nat. Nanotechnol. **2009**, 4, 315–319
- ³⁴ Ho, J. C.; Yerushalmi, R.; Jacobson, Z. A.; Fan, Z.; Alley, R. L.; Javey, A. Controlled nanoscale doping of semiconductors via molecular monolayers Nat. Mater. **2008**, 7, 62-67
- ³⁵ Xie, P.; Hu, Y.; Fang, Y.; Huang, J.; Lieber, C. M. Diameter-dependent dopant location in silicon and germanium nanowires Proc. Natl. Acad. Sci. **2009**, 106, 15254-15258
- ³⁶ Koren, E.; Berkovitch, N.; Rosenwaks, Y. Measurement of active dopant distribution and diffusion in individual silicon nanowires Nano Lett. **2010**, 10, 1163-1167
- ³⁷ Allen, J. E.; Perea, D. E.; Hemesath, E. R.; Lauhon, L. J. Nonuniform nanowire doping profiles revealed by quantitative scanning photocurrent microscopy Adv. Mater. **2009**, 21, 3067-3072
- ³⁸ Glas, F. Critical dimensions for the plastic relaxation of strained axial heterostructures in free-standing nanowires Phys. Rev. B **2006**, 74, 121302
- ³⁹ Galopin, E.; Largeau, L.; Patriarche, G.; Travers, L.; Glas, F.; Harmand, J. C. Morphology of self-catalyzed GaN nanowires and chronology of their formation by molecular beam epitaxy Nanotechnol. **2011**, 22, 245606
- ⁴⁰ May, B. J.; Selcu, C. M.; Sarwar, A. T. M. G.; Myers, R. C. Nanoscale current uniformity and injection efficiency of nanowire light emitting diodes Appl. Phys. Lett. **2018**, 112, 093107

⁴¹ Kent, T. F.; Carnevale, S. D.; Sarwar, A. T.; Phillips, P. J.; Klie, R. F.; Myers, R. C. Deep ultraviolet emitting polarization induced nanowire light emitting diodes with Al_xGa_{1-x}N active regions *Nanotechnol.* **2014**, *25*, 455201.

⁴² Basanta, R.; Mahesh, K.; Mohana, K. R.; Thirumaleshwara N. B.; Krupanidhi, S. B. Binary group III-nitride based heterostructures: band offsets and transport properties *J. Phys. D: Appl. Phys.*, **2015**, *48*, 423001

⁴³ Ebaid, M.; Min, J.; Zhao, C.; Ng, T. K.; Idriss, H; Ooi, B. S. Water Splitting over Epitaxially Grown InGa_N Nanowires on-Metallic Titanium/Silicon Template: Reduced Interfacial Transfer Resistance and Improved Stability *J. Mater. Chem. A* **2018** DOI: 10.1039/C7TA11338B

⁴⁴ Priante, D.; Janjua, B.; Prabaswara, A.; Subedi, R. C.; Elafandy, R. T.; Lopatin, S.; Anjum, D. H.; Zhao, C.; Ng, T. K.; Ooi, B. S. Highly uniform ultraviolet-A quantum-confined AlGa_N nanowire LEDs on metal/silicon with a TaN interlayer *Opt. Mater. Exp.* **2017**, *7*, 4214-4224

⁴⁵ Janjua, B.; Sun, H.; Zhao, C.; Anjum, D. H.; Priante, D.; Alhamoud, A. A.; Wu, F.; Li, X.; Albadri, A. M.; Alyamani, A. Y.; El-Desouki, M. M.; Ng, T. K.; Ooi, B. S. Droop-free Al_xGa_{1-x}N/Al_yGa_{1-y}N quantum-disks-in-nanowires ultraviolet LED emitting at 337 nm on metal/silicon substrates *Opt. Exp.* **2017**, *25*, 1381–1390

⁴⁶ Sun, H.; Shakfa, M. K.; Muhammed, M.; Janjua, B.; Li, K. H.; Lin, R.; Ng, T. K.; Roqan, I. S.; Ooi, B. S.; Li, X. Surface-Passivated AlGa_N Nanowires for Enhanced Luminescence of Ultraviolet Light Emitting Diodes *ACS Photonics* **2018**, *5*, 964–970

⁴⁷ Janjua, B.; Sun, H.; Zhao, C.; Anjum, D. H.; Wu, F.; Alhamoud, A. A.; Li, X.; Albadri, A. M.; Alyamani, A. Y.; El-Desouki, M. M.; Ng, T. K.; Ooi, B. S. Self-planarized quantum-disks-in-nanowires ultraviolet-B emitters utilizing pendeo-epitaxy *Nanoscale* **2017**, *9*, 7805–7813

⁴⁸ Chang, J.-Y.; Chang, H.-T.; Shih, Y.-H.; Chen, F.-M.; Huang, M.-F.; Kuo, Y.-K. Efficient Carrier Confinement in Deep-Ultraviolet Light-Emitting Diodes With Composition-Graded Configuration *IEEE Trans. Electron Devices* **2017**, *64*, 4980–4984

⁴⁹ Zhang, Z. H.; Huang Chen, S. W.; Zhang, Y.; Li, L.; Wang, S.W.; Tian, K.; Chu, C.; Fang, M.; Kuo, H. C.; Bi, W. Hole transport manipulation to improve the hole injection for deep ultraviolet light-emitting diodes *ACS Photonics* **2017**, *4*, 1846–1850

⁵⁰ Zhang, Z. H.; Li, L.; Zhang, Y.; Xu, F.; Shi, Q.; Shen, B.; Bi, W. On the electric-field reservoir for III-nitride based deep ultraviolet light-emitting diodes *Opt. Exp.* **2017**, *25*, 16550-16559

⁵¹ Liang, Y.H.; Towe, E. Progress in efficient doping of high aluminum-containing group III-nitrides. *Appl. Phys. Rev.*, **2018** *5*, 011107

- ⁵² Wang, Q.; Connie, A. T.; Nguyen, H. P. T.; Kibria, M. G.; Zhao, S.; Sharif, S.; Shih, I.; Mi, Z. Highly efficient, spectrally pure 340 nm ultraviolet emission from $\text{Al}_x\text{Ga}_{1-x}\text{N}$ nanowire based light emitting diodes *Nanotechnol.* **2013**, 24, 345201
- ⁵³ Zhao, S.; Connie, A. T.; Dastjerdi, M. H. T.; Kong, X. H.; Wang, Q.; Djavid, M.; Sadaf, S.; Liu, X. D.; Shih, I.; Guo, H.; Mi, Z. Aluminum nitride nanowire light emitting diodes: Breaking the fundamental bottleneck of deep ultraviolet light sources *Sci. Rep.* **2015**, 5, 8332
- ⁵⁴ Kazarino, R. F.; Tsarenkov, G. V. Theory of a variable-gap laser *Sov. Phys. Semicond.* 1976, 10, 178–182
- ⁵⁵ Tsang, W. T. A graded-index waveguide separate-confinement laser with very low threshold and a narrow Gaussian beam *Appl. Phys. Lett.* **1981**, 39, 134–137
- ⁵⁶ Tsang, W. T. Extremely low threshold (AlGa)As modified multiquantum well heterostructure lasers grown by molecular beam epitaxy *Appl. Phys. Lett.* **1981**, 39, 786
- ⁵⁷ Kasemset, D.; Hong, C.-S.; Patel, N. B.; Dapkus, P. D. Graded barrier single quantum well lasers - Theory and experiment *IEEE J. Quantum Electron.* **1983**, 19, 1025
- ⁵⁸ Shatalov, M.; Sun, W.; Lunev, A.; Hu, X.; Dobrinsky, A.; Bilenko, Y.; Yang, J.; Shur, M.; Gaska, R.; Moe, C.; Garrett, G.; Wraback, M. AlGa_N Deep-Ultraviolet Light-Emitting Diodes with External Quantum Efficiency above 10% *Appl. Phys. Express* **2012**, 5, 082101
- ⁵⁹ Sun, H.; Woodward, J.; Yin, J.; Moldawer, A.; Pecora, E. F.; Nikiforov, A.Y.; Dal Negro, L.; Paiella, R.; Ludwig Jr, K.; Smith, D. J.; and Moustakas, T. D. Development of AlGa_N-based graded-index-separate-confinement-heterostructure deep UV emitters by molecular beam epitaxy *J. Vac. Sci. Technol. B* **2013**, 31(3), p.03C117
- ⁶⁰ Janjua, B.; Sun, H.; Zhao, C.; Anjum, D. H.; Wu, F.; Alhamoud, A. A.; Li, X.; Albadri, A. M.; Alyamani, A. Y.; El-Desouki, M. M.; Ng, T. K.; Ooi, B. S. Self-planarized quantum-disks-in-nanowires ultraviolet-B emitters utilizing pendeo-epitaxy. *Nanoscale* **2017**, 9, 7805– 7813
- ⁶¹ Stańczyk, S.; Czyszanowski, T.; Kafar, A.; Goss, J.; Grzanka, S.; Grzanka, E.; Czernecki, R.; Bojarska, A.; Targowski, G.; Leszczyński, M.; Suski, T.; Kucharski, R.; Perlin, P. Graded-index separate confinement heterostructure InGa_N laser diodes *Appl. Phys. Lett.* **2013**, 103, 261107
- ⁶² Pecora, E. F.; Sun, H.; Negro, L. D.; Moustakas, T. D. Deep-UV optical gain in AlGa_N-based graded-index separate confinement heterostructure *Opt. Mater. Exp.* **2015**, 5, 809
- ⁶³ Sun, H.; Yin, J.; Pecora, E. F.; Negro, L. D.; Paiella, R.; Moustakas, T. D. Deep-Ultraviolet Emitting AlGa_N Multiple Quantum Well Graded-Index Separate-Confinement Heterostructures Grown by MBE on SiC Substrates *IEEE Photon. J.* **2017**, 9, 2201109

⁶⁴ Brunner, D.; Angerer, H.; Bustarret, E.; Freudenberg, F.; Höpler, R.; Dimitrov, R.; Ambacher, O.; Stutzmann, M. Optical constants of epitaxial AlGa_N films and their temperature dependence J. Appl. Phys. **1997**, 82, 5090-5096

⁶⁵ Frost, T.; Jahangir, S.; Stark, E.; Deshpande, S.; Hazari, A.; Zhao, C.; Ooi, B. S.; Bhattacharya, P. Monolithic electrically injected nanowire array edge-emitting laser on (001) silicon Nano Lett. **2014**, 14, 4535-4541

⁶⁶ Jahangir, S.; Frost, T.; Hazari, A.; Yan, L.; Stark, E.; LaMountain, T.; Millunchick, J. M.; Ooi, B. S.; Bhattacharya, P. Small signal modulation characteristics of red-emitting (λ = 610 nm) III-nitride nanowire array lasers on (001) silicon Appl. Phys. Lett. **2015**, 106, 071108

For Table of Contents Use Only (TOC)

Graded-Index Separated Confinement Heterostructure AlGaIn Nanowires: Towards Ultraviolet Laser Diodes Implementation

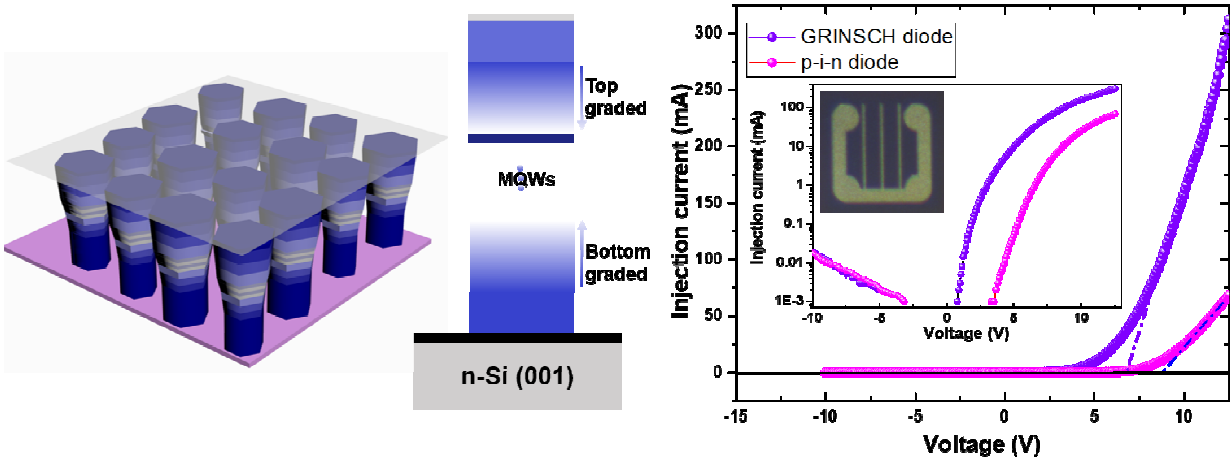
Haiding Sun^{1#}, Davide Priante², Jung-Wook Min², Ram Chandra Subedi², Mohammad Khaled Shakfa², Zhongjie Ren¹, Kuang-Hui Li¹, Ronghui Lin¹, Chao Zhao², Tien Khee Ng², Jae-Hyun Ryou³, Xixiang Zhang⁴, Boon S. Ooi^{2##}, Xiaohang Li^{1, ###}

¹ King Abdullah University of Science & Technology (KAUST), Computer, Electrical, and Mathematical Sciences and Engineering Division, Advanced Semiconductor Laboratory, Thuwal 23955-6900, Saudi Arabia

² King Abdullah University of Science & Technology (KAUST), Computer, Electrical, and Mathematical Sciences and Engineering Division, Photonics Laboratory, Thuwal 23955-6900, Saudi Arabia

³ Department of Mechanical Engineering, Material Science and Engineering Program, Texas Center for Superconductivity at UH (TcSUH), and Advanced Manufacturing Institute (AMI), University of Houston, Houston, TX, 77204-4006, USA

⁴ Division of Physical Science and Engineering, King Abdullah University of Science and Technology, Thuwal 23955-6900, Saudi Arabia



A 3D schematic depiction of the fabricated nanowire GRINSCH UV emitters and the I-V curves of the GRINSCH and conventional p-i-n diodes.